Assessment of Low-Cost GNSS Receiver Performance in Urban Environments

Giuseppina Vacca(✉), Enrica Vecchi, and Antonio Pala

Department of Civil, Environmental Engineering and Architecture, University of Cagliari, Cagliari 09123, Italy
{giuseppina.vacca,vaccag}@unica.it

Abstract. Global Navigation Satellite System (GNSS) enables positioning accuracies ranging from meter-level to sub-centimeter, traditionally achieved using geodetic-grade receivers. However, the high cost of such instruments still limits their accessibility in many practical applications. In this context, the recent development of multi-frequency, multi-constellation low-cost GNSS receivers has opened new perspectives for cost-effective high-precision positioning, although their performance in challenging environments remains to be fully assessed. This study evaluates the performance of a multi-frequency low-cost (LC) GNSS receiver (u-blox ZED-F9P with ANN-MB-00 patch antenna) in comparison with a geodetic-grade device (GD), Trimble R12. Experiments were conducted in two representative urban environments: a semi-open area (ST1) and an obstructed area characterized by buildings and vegetation (ST2). Both static relative positioning and Network Real-Time Kinematic (NRTK) techniques were investigated, using the geodetic receiver as a reference. Signal quality was assessed in terms of carrier-to-noise ratio (C/N_0) and multipath (MP) errors. In static positioning, millimeter-level agreement with the geodetic solution is achieved in horizontal components under favorable conditions, while errors increase to the centimeter level in obstructed environments. The NRTK results confirm this behavior, with sub-centimeter horizontal dispersion in semi-open conditions and a degradation up to the centimeter level in the obstructed environment. The vertical component consistently exhibits the largest errors, with systematic biases and higher variability, confirming its greater sensitivity to environmental effects. Overall, the results highlight the potential of multi-frequency LC GNSS receivers for high-precision applications under favorable conditions, while emphasizing their sensitivity to multipath and signal obstruction in urban environments.

Keywords: GNSS · low-cost receivers · u-blox · NRTK · urban surveying

1 Introduction

Global Navigation Satellite System (GNSS) technology has been widely used for many years across a broad range of applications, from navigation to high-precision static positioning, with achievable accuracy ranging from a few meters down to the sub-centimeter levels [1].

© The Author(s), under exclusive license to Springer Nature Switzerland AG 2027
O. Gervasi et al. (Eds.): ICCSA 2026 Workshops, LNCS 16766, pp. 86–103, 2027.
https://doi.org/10.1007/978-3-032-30539-8_6

In particular, the concept of high-precision GNSS positioning, for both post-processing and real-time applications, has traditionally been associated with geodetic-grade receivers, which are characterized by high performance, robustness, and well-established reliability. However, despite their widespread availability on the market, the cost of such equipment remains high, limiting its accessibility for many users, especially in application fields where cost-effectiveness is a primary concern.

In this context, low-cost receivers have been progressively developed, initially based on single-frequency modules [2]. As expected, the lack of dual-frequency observations at that stage constrained their performance, both in terms of accuracy and operational capabilities [3].

In parallel, recent years have undergone the rapid expansion and full operational capability of multiple GNSS constellations, resulting in a substantial increase in the number of available satellites. At present, more than 110 satellites are operational across four different constellations, 99 of which are in the Medium Earth Orbit (MEO): GPS (29), GLONASS (24), Galileo (22), and BeiDou (24). Consequently, multi-constellation positioning based on a large number of simultaneously visible satellites has rapidly become a common scenario [4].

This technological evolution has significantly driven the development of GNSS instruments, particularly in the low-cost market. Indeed, modern low-cost devices now support multi-frequency, multi-constellation observations and are often equipped with Real-Time Kinematic (RTK) and Network RTK (NRTK) capabilities. These features have made low-cost instruments suitable for precise positioning in a wide range of geodetic and surveying applications [1]. As a result, it is now feasible to assemble low-cost GNSS systems based on OEM (Original Equipment Manufacturer) modules, offering a cost-effective alternative to commercial geodetic receivers currently available on the market. The price difference is notable, with low-cost receivers typically costing a few hundred euros, compared to over 10 k–15 k euros for geodetic devices.

Another key distinction between low-cost GNSS receivers and geodetic-grade instruments lies in the way they are delivered to users. Low-cost receivers are typically provided as modular components that require ad hoc assembly and integration to form a fully operational setup, while geodetic-grade receivers are generally supplied as complete, ready-to-use solutions.

Several studies have investigated the design and performance of multi-frequency low-cost GNSS (MF-LC GNSS) receivers. Commercial devices such as u-blox, Emlid, Sky-Traq, Swift, and Piksi Multi have demonstrated the capability of achieving centimeter-level accuracy, particularly in open and rural environments [3, 5, 6]. In such environments, relative positioning solutions can achieve optimal accuracies, reaching up to 1 mm in the horizontal components and 3 mm in height [7, 8]. However, the scientific literature addressing GNSS performance in urban or densely vegetated environments remains relatively limited [9].

The present study aims to evaluate the performance of a multi-frequency (MF) low-cost (LC) GNSS receiver under urban and obstructed conditions, with particular emphasis on its comparison with a geodetic-grade device (GD). Specifically, the u-blox ZED-F9P MF-LC receiver, equipped with the u-blox ANN-MB-00 antenna, was adopted as the

low-cost solution, while a Trimble R12 receiver was used as a reference to assess positioning accuracy and overall performance. The low-cost receiver costs approximately 400 euros, while the geodetic-grade receiver exceeds 15,000 euros.

The remainder of the paper is organized as follows: Sect. 2 presents the instrumentation, study area, and experimental setup; Sect. 3 reports the results; and Sect. 4 provides a discussion of the results and the main conclusions.

2 Materials and Methods

2.1 GNSS Devices

Low-Cost Receiver

In this study, a low-cost GNSS receiver, the ZED-F9P-02B (hereafter referred to as "LC"), was employed: This device integrates multi-band Real-Time Kinematic (RTK) technology, enabling centimeter-level positioning accuracy under favorable conditions. The very compact size of the module (17.0 × 22.0 × 2.4 mm) makes it suitable for several applications. The ZED-F9P-02B supports multi-constellation and multi-frequency signal tracking, including GPS (L1 C/A, L2C), GLONASS (L1OF, L2OF), Galileo (E1, E5b), and BeiDou (B1I, B2I). This multi-band capability improves robustness against multipath and enhances ambiguity resolution performance compared to single-frequency receivers. Detailed specifications are available at [10].

The LC receiver was combined with a compact and versatile multi-band patch antenna, the ANN-MB-00-00, also produced by u-blox, as shown in Fig. 1.

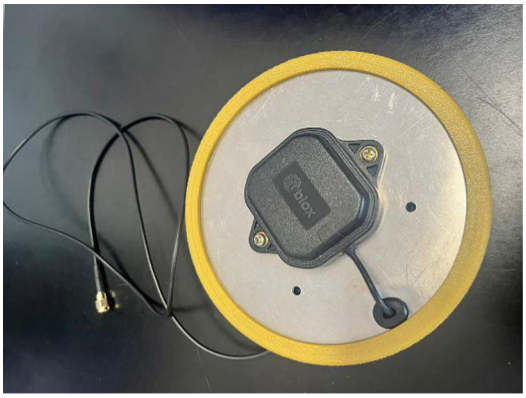

Fig. 1. u-blox ANN-MB-00-00 multi-band antenna mounted on a 3D-printed ground plane.

To ensure optimal signal reception and proper functionality, the antenna was mounted on a custom 3D-printed ground plane, providing a stable reference surface and minimizing potential interference from surrounding components (Fig. 1). This antenna provides stable performance across multi-frequency and is well suited for integration with the ZED-F9P-02B module. Additional specifications are available at [11].

Geodetic Receiver

For validation purposes, a geodetic-grade GNSS receiver (Trimble R12), hereafter referred to as "GD", was used to define the ground truth. The Trimble R12 is a high-performance multi-frequency, multi-constellation receiver equipped with 672 channels, capable of tracking GPS, GLONASS, Galileo, BeiDou, and QZSS signals. It is designed for professional surveying applications and provides robust RTK performances, and enhanced resistance to challenging environments such as multipath and signal obstruction [12].

2.2 Study Area

The study area is located within the Faculty of Engineering and Architecture of the University of Cagliari (Sardinia, Italy). Two test environments representative of typical urban surveying conditions were selected (Fig. 2), reflecting contexts in which completely open-sky scenarios are rarely encountered. These environments are hereafter referred to as "ST1" and "ST2".

- ST1: semi-open environment, with limited obstructions from surrounding buildings or vegetation and relatively good sky visibility. The survey point in ST1 is located on a flat paved courtyard, surrounded by Faculty buildings (approximately 5–10 m in height) and sparse tall trees. Both types of obstacles are sufficiently distant from the observation point to preserve adequate sky visibility.
- ST2: obstructed area, affected by the combined presence of buildings and dense tall trees. The survey point in ST2 is located along a flat passageway crossing a tree-lined courtyard. In this case, the primary source of obstruction is represented by the surrounding vegetation, while Faculty buildings (with heights comparable to those in ST1) are also present at greater distances from the observation point.

At each site, two nearby survey points (denoted as ST' and ST") were established. These points were positioned as close as possible to each other while still allowing sufficient space for tripod installation (approximately 70 cm separation), as shown in Fig. 3. This configuration ensures comparable satellite geometry and visibility conditions at both points, thus minimizing differences related to instruments placement.

2.3 Quality Control of GNSS Observations

Low-cost GNSS receivers generally exhibit lower performance compared to geodetic-grade receivers, primarily due to differences in hardware design [3, 13, 14]. To assess GNSS observation quality, the carrier-to-noise ratio (C/N_0) and multipath error (MP) were considered as the primary metrics. Low-cost receivers typically exhibit lower C/N_0 values due to reduced signal tracking performance [5, 14]. This effect can be assessed by analyzing corresponding observations collected using both LC and GD receivers under semi-open sky (ST1) and obstructed (ST2) conditions. For geodetic receivers, C/N_0 values generally range between 35–45 dB-Hz, decreasing below 30 dB-Hz at low elevation angles [15].



Fig. 2. Map of the survey points, showing ST1 and ST2, and the UCAG permanent GNSS station located on the rooftop of the Faculty of Engineering building at the University of Cagliari. Grid coordinates are aligned to WGS84 system (EPSG:4326), basemap is derived from Google Satellite imagery.

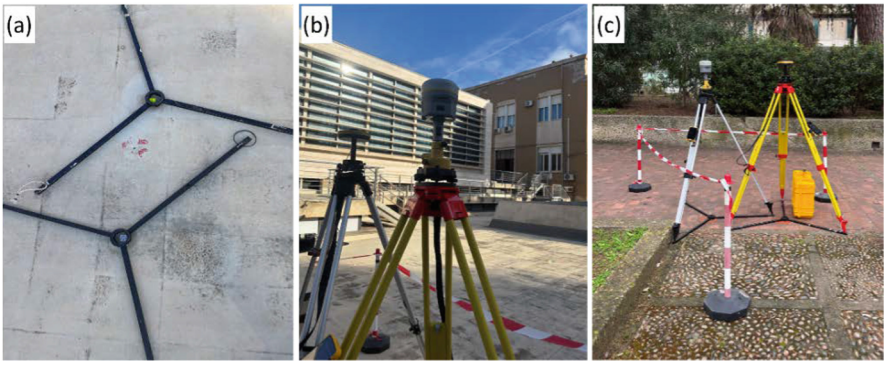

Fig. 3. Configuration of the two nearby survey points (ST' and ST"), illustrated for the ST1 environment (a), and setup of the two GNSS receivers operating at ST1 (b) and ST2 (c).

Multipath errors, meaning the effects occurring when the GNSS signal received by the antenna results from the superposition of direct and reflected (or refracted) components, are strongly environment-dependent due to the presence of surrounding objects (buildings, terrain, and vegetation) [16]. Moreover, since multipath implies that both direct and reflected signals enter the receiver through the antenna, mitigation strategies often focus on antenna design, which represent one of the main parameters affecting its final effect [17, 18]. For instance, specialized antennas such as right-handed circularly polarized or Choke-Ring designs are commonly employed to mitigate multipath effects [19]. Low-cost antennas, by contrast, are generally more susceptible due to their reduced

ability to discriminate against reflected signals, also because they are commonly provided without dedicated design support. The issue is particularly pronounced in urban and vegetated environments, where dense reflective surfaces and foliage increase signal scattering, ultimately leading to degradation in positioning accuracy [20].

The chosen configuration of the survey points (see Sect. 2.2), with LC and GD receivers installed approximately 70 cm apart, allowed the evaluation of these factors under identical observation conditions.

2.4 GNSS Positioning and Data Processing

Static Sessions

The positioning accuracy of the low-cost (LC) receiver was assessed by comparison with the geodetic-grade (GD) receiver operating at the same survey point. Thus, for each environment (semi-open sky and obstructed area), two independent datasets were collected, with the GD providing the ground truth. Measurement sessions were conducted one day apart to ensure similar environmental and satellite conditions. This experimental design was necessary because each survey point had to be independently validated using the GD receiver.

The acquisition scheme is summarized as follows:

Semi-open environment - ST1

- Session 1A
  - Point ST1' → GD
  - Point ST1" → LC
- Session 1B (instrument swap, one day apart):
  - Point ST1' → LC
  - Point ST1" → GD

Obstructed area environment - ST2

- Session 2A:
  - Point ST2' → GD
  - Point ST2" → LC
- Session 2B (instrument swap, one day apart):
  - Point ST2' → LC
  - Point ST2" → GD

A common observation interval shared by all sessions across both environments (ST1 and ST2) was selected, resulting in an overlapping duration of approximately 4 h. Although the first two sessions were originally longer, they were truncated to ensure

Table 1. GNSS acquisition sessions at ST1 and ST2, showing session IDs, and overlapping observation time intervals (UTC), with start and stop times of each acquisition.

Environment	Session	Observation time	
		Start (UTC)	Stop (UTC)
Semi-open ST1	1A – day 1	08:29:46	15:10:36
	1B – day 2	08:31:22	14:44:53
Obstructed ST2	2A – day 1	08:35:40	12:35:51
	2B – day 2	08:22:12	12:24:16

consistency and comparability across all datasets under similar observational conditions (Table 1).

Positioning was performed using baselines computed with respect to the UCAG (UCAG00ITA) permanent GNSS station, located on the rooftop of the Engineering building of the University of Cagliari. The UCAG station, operated by the Italian Space Agency (ASI) [21], has been included in the European Permanent Network (EPN) since August 2015 and is classified as Class A station. As such, it provides a stable and reliable reference for high-precision GNSS positioning and baseline analysis.

Due to the short distance between the survey points and the reference station (<1 km), all baselines (ST1'- UCAG, ST1"- UCAG, ST2'- UCAG, ST2"- UCAG) can be classified as short baselines.

Data processing was performed using the open-source software RTKLIB-EX (version 2.5.0) [22], with parameters summarized in Table 2. Coordinates (E, N, h) were computed in the official national reference system ETRS89/ETRF2000, and positioning errors were assessed by comparing the LC-derived coordinates with the GD reference solution.

Table 2. Main parameters adopted for static GNSS processing using RTKLIB.

Parameter	Value
Signal frequencies	Dual frequency
GNSS Constellations	GPS, GLONASS, Galileo, BeiDou, SBAS
Elevation mask	15 deg
Sampling interval	15 s
Tropospheric model	Saastamoinen
Ionospheric model	Broadcast
Ephemerides	Broadcast

NRTK Sessions

Additional tests were conducted using the LC receiver in NRTK (Network Real-time

Kinematic) mode. Corrections were provided by the Sardinian permanent GNSS network SARNET [23], ensuring alignment with the ETRF2000-UTM32N coordinate system (EPSG: 6707).

In particular, the performance of the LC receiver in NRTK mode was evaluated through repeated short-duration sessions designed to simulate real operational conditions. Measurements were carried out on two consecutive days, at one point for each environment, following the same acquisition strategy to ensure consistency and comparability between the two scenarios.

The receiver remained continuously active during the observation period, while individual points were acquired at regular 15-min intervals, in order to assess temporal variability under changing satellite geometry conditions. The same time window adopted for the static sessions was used for consistency (approximately between 09:00 and 13:00 UTC), with 5 s observations, resulting in 17 independent measurements for each environment. The antenna was mounted on a 2 m survey pole, properly centered over the point and stabilized using a bipod (Fig. 4), ensuring adequate centering and leveling stability throughout the entire observation period.



Fig. 4. GNSS antenna setup with bipod support during the NRTK measurements (ST1).

3 Results

3.1 Carrier-to-Noise Ratio (C/N_0) Analysis

This section presents the analysis of the carrier-to-noise ratio (C/N_0) as a primary indicator of signal quality, comparing the low-cost (LC) and geodetic-grade (GD) receivers under the two selected different environmental conditions. The comparison is performed

between the two frequency bands (L1 and L2), considering all tracked constellations together. In the L1 band, signals such as L1 C/A, L1OF, E1, and B1I are included, while in the L2 band signals such as L2C, L2OF, E5b, and B2I are considered.

For clarity, results are presented for only one representative point per session, reflecting the corresponding environmental conditions (semi-open and obstructed). Figures 5 and 6 depict the Carrier-to-noise ratio (C/N_0) as a function of satellite elevation angle for the LC and GD receivers, respectively, based on RTKLIB processing, while Table 3 summarizes the main results.

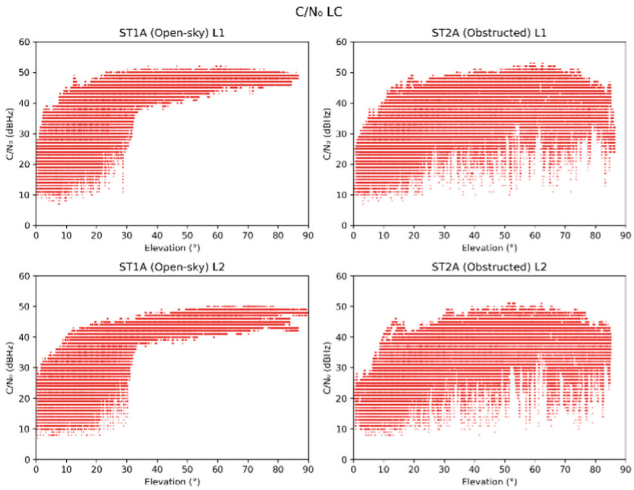

Fig. 5. C/N_0 for LC receiver as a function of satellite elevation angle.

Observing the C/N_0 graphs in Figs. 5 and 6 as a function of satellite elevation angle for LC and GD receivers, respectively, and considering the statistical summary in Table 3, the following trends can be identified:

- **LC vs GD:** the geodetic receiver consistently exhibits higher SNR values compared with the low-cost receiver, indicating superior signal tracking performance and measurement stability. The LC receiver shows a higher variability (higher Std value), resulting in more sparse distribution.
- **L1 vs L2:** for both receivers, L1 signals show slightly higher values compared to L2, confirming the generally better signal quality and robustness of the L1 frequency, however, this small variation is not clearly noticeable in the distributions and becomes evident primarily from the statistical results.
- **ST1 vs ST2:** a clear degradation in C/N_0 is observed in the obstructed environment (ST2), with a more pronounced reduction for the low-cost receiver, highlighting its higher sensitivity to signal attenuation. In particular, the mean value decreases by approximately 7.9% for the geodetic receiver and 8.8% for the low-cost receiver from ST1 to ST2.

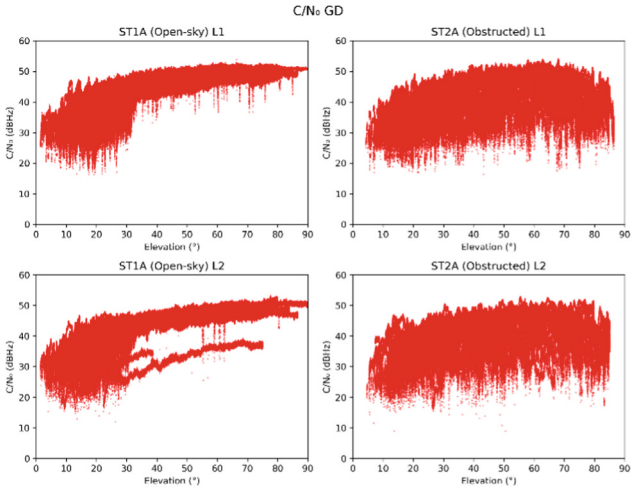

Fig. 6. C/N_0 for GD receiver as a function of satellite elevation angle.

Table 3. Statistical summary of C/N_0 values for the LC and GD receivers, reported for one session in ST1 (S1A) and one in ST2 (S2A), for both frequencies. Mean, median, and standard deviation (Std) are provided; all values are expressed in dB-Hz.

Receiver	Session	Frequency	Mean	Median	Std
GD	S1A	L1	44.5	46.4	6.1
	S1A	L2	42.7	44.7	6.1
	S2A	L1	41.0	41.7	6.4
	S2A	L2	39.9	40.6	6.0
LC	S1A	L1	41.9	45.0	7.6
	S1A	L2	38.7	42.0	8.0
	S2A	L1	38.2	39.0	8.1
	S2A	L2	36.0	38.0	7.8

3.2 Multipath Effects

The multipath error analysis is reported in this subsection, with the aim of evaluating the impact of antenna quality and surrounding environment on signal reflections and measurement distortions. As in the previous case, only one representative point from each session is presented. Figures 7 and 8 show the multipath errors for the LC and GD receivers, respectively, plotted against the satellite elevation angle, and Table 4 summarizes the main results.

Based on the multipath distributions shown in Figs. 7 and 8 for the LC and GD receivers, together with the statistical summary reported in Table 4, the main observed trends are summarized as follows:

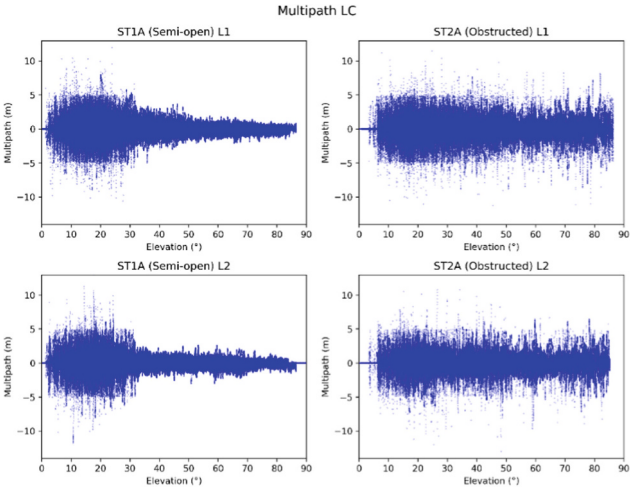

Fig. 7. Multipath LC.

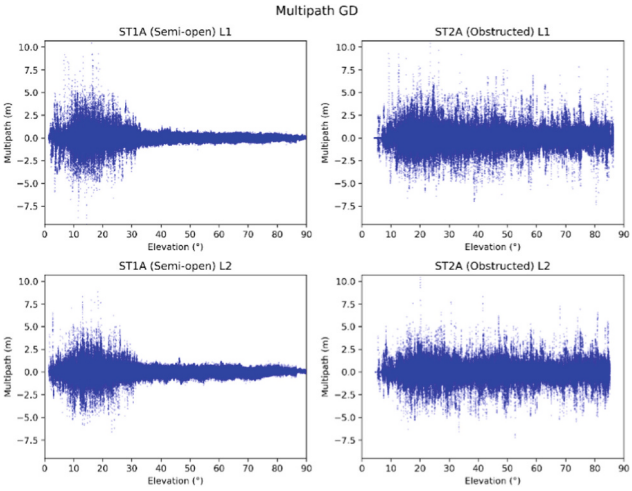

Fig. 8. Multipath GD.

- **LC vs GD:** the LC receiver exhibits significantly higher (about two times) multipath levels compared with the geodetic receiver, primarily due to the lower quality of the antenna system which is known to be the major factor affecting this parameter [18].
- **L1 vs L2:** minor differences are observed between L1 and L2 under the same environmental conditions.
- **ST1 vs ST2:** multipath effects increase substantially in the obstructed environment, confirming the strong influence of surrounding obstacles such as vegetation and buildings. The trend is clearly visible both in the graphs and in the statistical results. In

Table 4. Statistical summary of MP values for the LC and GD receivers, reported for one session in ST1 (S1A) and one in ST2 (S2A), for both L1 and L2 frequencies. Standard deviations (Std) are provided, with values expressed in meters.

Receiver	Session	L1 Std	L2 Std
GD	S1A	0.46 m	0.47 m
GD	S2A	0.82 m	0.80 m
LC	S1A	0.88 m	0.87 m
LC	S2A	1.21 m	1.14 m

particular, the standard deviation increases by approximately 70–78% for the geodetic receiver and 31–38% for the low-cost receiver from ST1 to ST2.

It is worth noting that multipath levels for a GD receiver are typically lower in fully open-sky conditions than those observed at ST1. Indeed, ST1 is a semi-open environment, where nearby buildings and vegetation introduce residual reflections (Figs. 2 and 3).

3.3 Positioning Accuracy

Static Positioning

Static positioning performance is assessed by comparing the coordinates estimated by the LC receiver with those obtained from the GD, which is used as reference. The influence of environmental conditions is also evaluated by comparing results in ST1 and ST2.

For each dataset, the static solution is computed as the mean of all available epochs over the entire observation period (approximately 4 h), using RTKLIB software with the parameters listed in Table 2. Based on these positions, coordinate differences between LC and GD solutions are calculated for the Easting (E), Northing (N), and ellipsoidal height (h) components. These differences represent the positioning bias and are used as indicators of accuracy with respect to the reference solution. In addition, the solution quality (Q) and the number of tracked satellites are examined to further assess the reliability of the positioning results under the two environmental conditions. A three-dimensional error metric is computed as the Euclidean distance between the LC and GD coordinates, representing the overall positioning error derived from the averaged solutions.

Table 5 summarizes the comparison between the GD and LC solutions for the two environments. In ST1, the LC-GD differences are at the millimeter level in the horizontal components, while the vertical component shows a difference of about 1.3 cm. The resulting horizontal error is approximately 3 mm, while the 3D error remains at the centimeter level, confirming a high level of agreement between the two receivers under favorable conditions.

In both environments, fixed solutions ($Q = 1$) are achieved by both receivers, despite differences in the number of tracked satellites. In ST2, the discrepancies increase, particularly in the Northing component (1.6 cm), while the Easting difference remains limited

Table 5. Comparison of LC and GD static solutions in ST1 and ST2. The quality indicator (Q), number of satellites (NS), coordinate differences (LC - GD, in meters), and horizontal and 3D errors are reported.

Env	Q_GD	NS_GD	Q_LC	NS_LC	dE (m)	dN (m)	dh (m)	error hor	error 3D
ST1	1	17	1	17	−0.002	0.002	−0.013	0.003	0.013
ST2	1	13	1	18	0.002	0.016	−0.031	0.016	0.035

(2 mm) and comparable to the values observed in ST1. The vertical component shows a larger bias of about 3.1 cm. Consequently, the horizontal error rises to approximately 1.6 cm, and the 3D error reaches about 3.5 cm, indicating a degradation in positioning performance. These results suggest that, although fixed ambiguity solutions are maintained in both environments, positioning accuracy decreases under more challenging conditions, likely due to increased multipath effects and signal obstructions, with a more pronounced impact on the vertical component.

NRTK Performance

The positioning performance in NRTK mode was evaluated in terms of temporal stability, defined as the repeatability of the estimated coordinates over time and their sensitivity to variations in satellite geometry. The assessment was conducted using repeated short-duration observations acquired at regular time intervals, and the results were then compared with those obtained under static conditions. Furthermore, measurements collected in the two environments (ST1, ST2) were analyzed to investigate the influence of surrounding conditions on positioning performance.

Figure 9 illustrates the time series of the three position components during the NRTK session in ST1, together with their corresponding mean values and standard deviations. The horizontal components exhibit a good stability throughout the observation period, with standard deviations of 3.5 mm and 5.8 mm, for the Easting and Northing components, respectively. This results in a combined horizontal dispersion at the sub-centimeter level (less than 7 mm), with a slightly larger contribution from the Northing component.

The residuals of each epoch with respect to the corresponding mean value are generally contained within approximately ±0.01 m, indicating a stable and well-converged solution over time. The vertical component shows higher variability, with a standard deviation of approximately 1.4 cm over the 17 solutions considered. Consistently, the height residuals exhibit a wider dispersion compared to the horizontal components.

A notable outlier is observed in the vertical component, reaching approximately +0.042 m relative to the mean position, around 12:00 UTC. This deviation may be attributed to a temporary degradation in satellite geometry or multipath effects. Overall, this behavior is expected, as the vertical component in GNSS positioning is generally less precise due to the inherent satellite geometry and atmospheric influences.

Figure 10 illustrates the same analysis as Fig. 9, applied to the obstructed environment (ST2). Compared to ST1, a noticeably higher variability is observed in all components. The horizontal components show standard deviations of approximately 1.6 cm and 2.0 cm for Easting and Northing, respectively, resulting in a combined horizontal dispersion of

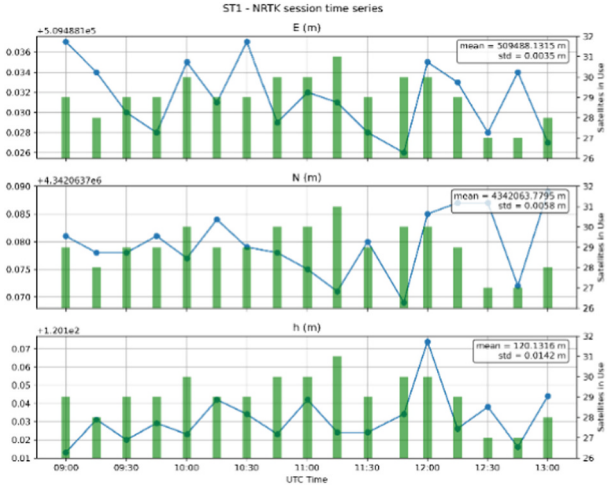

Fig. 9. NRTK time series in the semi-open environment (ST1) for Easting (E), Northing (N), and ellipsoidal height (h), together with the corresponding number of tracked satellites.

about 2.6 cm. This represents a significant degradation with respect to ST1, with the horizontal dispersion increasing by approximately three to four times

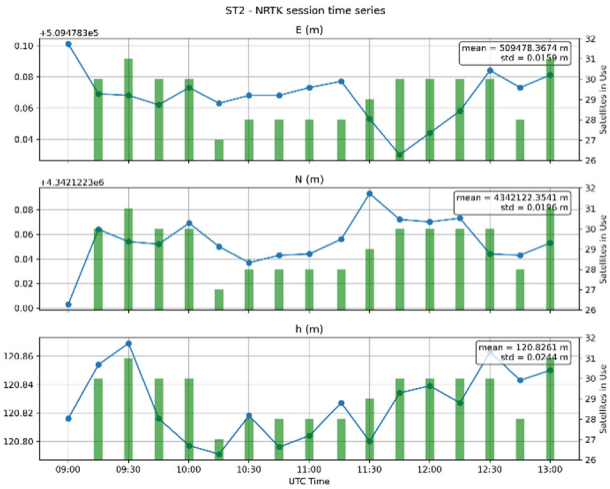

Fig. 10. NRTK time series in the obstructed environment (ST2) for Easting (E), Northing (N), and ellipsoidal height (h), together with the corresponding number of tracked satellites.

The residuals of each epoch with respect to the mean position are generally contained within ± 0.04 m, although several epochs exhibit larger deviations, particularly in the Northing component. This indicates a reduced positioning stability over time, despite all solutions being classified as fixed. The vertical component shows the highest variability,

with a standard deviation of approximately 2.4 cm, confirming the inherently lower precision of the height component in GNSS positioning.

Some noticeable deviations can be identified, especially in the later part of the session (after approximately 12:30 UTC), where both horizontal and vertical components exhibit increased dispersion. These variations are likely related to changes in satellite geometry and to the stronger influence of multipath effects in the obstructed environment, characterized by the presence of buildings and vegetation.

Across both ST1 and ST2, the number of satellites tracked remains relatively stable throughout the observation periods, with only minor variations (Figs. 9 and 10), suggesting no significant correlation between this parameter and the observed performance differences. Instead, the degradation in positioning performance is more plausibly attributed to environmental conditions, such as signal obstructions and multipath effects, as discussed in Sect. 3.2.

To further assess the positioning performance, the NRTK results were compared against the reference solution derived from the complete static session (approximately 4 h) acquired with the GD receiver (see Sect. 2.4). Residuals were computed for the three components as the differences between the NRTK-derived positions and the reference coordinates.

In the semi-open environment (ST1), the NRTK solutions exhibit a good horizontal accuracy, with mean residuals close to zero (−6.0 mm in Easting and − 8 mm in Northing), indicating limited systematic bias. The vertical component, however, exhibits a more pronounced offset, with a mean residual of approximately −6 cm, which dominates the overall 3D error.

In the obstructed environment (ST2), a degradation in performance is observed. The residuals increase in magnitude, especially in the Northing component, reflecting reduced accuracy and enhanced sensitivity to environmental conditions. The vertical component remains the dominant source of error, with a mean bias of approximately − 9 cm (Table 6).

Table 6. Mean residuals of the NRTK solutions with respect to the reference static solution for ST1 and ST2. Values are reported for the Easting (dE), Northing (dN), and ellipsoidal height (dh) components, expressed in meters.

Env	Mean dE (m)	Mean dN (m)	Mean dh (m)
ST1	−0.006	−0.008	−0.06
ST2	0.006	−0.020	−0.09

4 Discussion and Conclusions

The increasing availability of low-cost multi-frequency GNSS receivers has opened new opportunities for high-precision positioning in surveying and geospatial applications. However, their performance under varying environmental conditions, particularly in urban environments, has not yet been fully investigated.

In this context, the performance of a u-blox (LC) GNSS receiver equipped with its patch antenna is analyzed under two environmental conditions representative of typical urban surveying scenarios. Both relative static and Network Real-Time Kinematic (NRTK) positioning strategies are investigated, using positions obtained from long static sessions of a Trimble R12 geodetic device (GD) as a reference.

The analysis of signal quality indicators confirms that the low-cost receiver is more sensitive to environmental conditions compared to the geodetic-grade device. In particular, lower C/N_0 values and higher variability are observed for the LC receiver, especially in the obstructed environment (ST2). This behavior is consistent with the multipath analysis, which shows significantly higher MP values for the LC solution, mainly due to the lower quality of the antenna and its increased susceptibility to signal reflections. The degradation observed from ST1 to ST2 clearly highlights the strong impact of surrounding obstacles on GNSS signal quality. Despite these limitations, the static positioning results indicate that the LC receiver is capable of achieving high accuracy under favorable conditions. In the semi-open environment (ST1), the agreement with the geodetic receiver is at the millimeter level in the horizontal components and at the centimeter level in height. In the obstructed environment (ST2), although fixed solutions are still maintained, the positioning accuracy decreases, with errors reaching the centimeter level, particularly in the Northing and vertical components.

The NRTK analysis further emphasizes the influence of environmental conditions on positioning performance. In ST1, the low-cost receiver provides stable results, with sub-centimeter horizontal dispersion. In contrast, in ST2, a clear degradation is observed, with horizontal dispersion increasing to the centimeter level (approximately 3–4 times higher than in ST1). The vertical component consistently represents the main source of error in both environments, showing systematic biases (approximately -6 cm in ST1 and $-$ 9 cm in ST2) and higher variability.

Our results are fully consistent with the literature on low-cost GNSS receivers, reporting lower C/N_0 values, increased multipath effects, and NRTK performance degradation from millimeter-level accuracy in open-sky conditions to centimeter-level errors in urban environments. Overall, the results demonstrate that low-cost GNSS receivers can be reliably employed in several real-world surveying applications where sub-centimeter performance is not strictly required or where environmental conditions are quite favorable. For instance, these may include topographic and cadastral surveys in open or semi-environments. More recently, such devices have also been proposed for dynamic applications, such as autonomous vehicles and onboard systems for Unmanned Aerial Vehicles (UAV)-based surveying. In these scenarios, operational strategies play a key role in mitigating the observed limitations of low-cost devices, particularly regarding antenna selection and placement.

Future work will focus on a more detailed investigation of LC performance in NRTK mode, including kinematic scenarios, solution stability, ambiguity fixing, and convergence times. Different combinations of receivers and antennas will also be explored, with the aim of identifying optimal configurations for low-cost and high-precision GNSS applications.

Disclosure of Interests. The authors have no competing interests to declare that are relevant to the content of this article.

References

1. Hamza, V., Stopar, B., Sterle, O., et al.: Observations and positioning quality of low-cost GNSS receivers: a review. GPS Solut. **28**, 149 (2024). https://doi.org/10.1007/s10291-024-01686-8
2. Tsakiri, M., Sioulis, A., Piniotis, G.: The use of low-cost, single-frequency GNSS receivers in mapping surveys. Surv. Rev. **50**(358), 46–56 (2018). https://doi.org/10.1080/00396265.2016.1222344
3. Hamza, V., Stopar, B., Sterle, O., et al.: Recent advances and applications of low-cost GNSS receivers: a review. GPS Solut. **29**, 56 (2025). https://doi.org/10.1007/s10291-025-01815-x
4. Sanna, G., Pisanu, T., Garau, S.: Behavior of low-cost receivers in base-rover configuration with geodetic-grade antennas. Sensors. **22**, 2779 (2022). https://doi.org/10.3390/s22072779
5. Poluzzi, L., Tavasci, L., Corsini, F., Barbarella, M., Gandolfi, S.: Low-cost GNSS sensors for monitoring applications. Appl. Geomat. (2020). https://doi.org/10.1007/s12518-019-00268-5
6. Gumilar, I., Sidiq, T., Shihran, R., et al.: Developing and evaluating low-cost GNSS to monitor land subsidence in Bandung Basin. Appl. Geomat. **18**, 15 (2026). https://doi.org/10.1007/s12518-025-00668-w
7. Chen, M., et al.: Assessment of the real-time and rapid precise point positioning performance using geodetic and low-cost GNSS receivers. Remote Sens. **16**(8), 1434 (2024). https://doi.org/10.3390/rs16081434
8. Curone., D., et al.: An innovative low-power, low-cost, multiconstellation geodetic-grade global navigation satellite system reference station for the densification of permanent networks:the GREAT project. Sensors. **23**(13), 6032 (2023). https://doi.org/10.3390/s23136032
9. Hamza, V., Stopar, B., Sterle, O., Pavlovčič-Prešeren, P.: Low-cost dual-frequency GNSS receivers and antennas for surveying in urban areas. Sensors. **23**, 2861 (2023). https://doi.org/10.3390/s23052861
10. u-blox: ZED-F9P module (2026). https://www.u-blox.com/en/product/zed-f9p-module. Last Accessed 20 Mar 2026
11. u-blox: ANN-MB Series GNSS Antennas (2026). https://www.u-blox.com/en/product/ann-mb-series-gnss-antennas. Last Accessed 20 Mar 2026
12. Trimble: Trimble R12 GNSS receiver (2026). https://geospatial.trimble.com/en/products/hardware/trimble-r12. Last Accessed 20 Mar 2026
13. Romero-Andrade, R., Trejo-Soto, M.E., Vega-Ayala, A., et al.: Positioning evaluation of single- and dual-frequency low-cost GNSS receiver signals using PPP and static relative methods in urban areas. Appl. Sci. **11**(22), 10642 (2021)
14. Paziewski, J.: Multi-constellation single-frequency ionospheric-free precise point positioning with low-cost receivers. GPS Solut. (2022). https://doi.org/10.1007/s10291-021-01209-9
15. Ghizzo, E., Lesouple, J., Milner, C.: Assessing spoofing impact on GNSS receivers: carrier-to-noise density ratio (C/N_0) estimation. Signal Process. **241**, 110389 (2026). https://doi.org/10.1016/j.sigpro.2025.110389
16. Jiang, Y., Guo, C., Wang, J., Xu, R.: Multipath effects mitigation in offshore construction platform GNSS-RTK displacement monitoring using parametric temporal convolution network. Remote Sens. **17**(4), 601 (2025). https://doi.org/10.3390/rs17040601
17. Krzan, G., Dawidowicz, K., Paziewski, J.: Low-cost GNSS antennas in precise positioning: a focus on multipath and antenna phase center models. GPS Solut. **28**(3), 103 (2024). https://doi.org/10.1007/s10291-024-01645-3
18. Poluzzi, L., Gandolfi, S.: Performance of dual-frequency low-cost GNSS sensors for real-time monitoring. In: Geomatics and Geospatial Technologies. Communications in Computer and Information Science. Springer (2022). https://doi.org/10.1007/978-3-030-94426-1_18

19. Chen, J., et al.: Performance analysis of a GNSS multipath detection and mitigation method with two low-cost antennas in RTK positioning. IEEE Sensors J. **22**(6), 4827–4835 (2022). https://doi.org/10.1109/JSEN.2021.3068767
20. Hamza, V., Stopar, B., Sterle, O.: Testing the performance of multi-frequency low-cost GNSS receivers and antennas. Sensors. **21**(6), 2021 (2021). https://doi.org/10.3390/s21062029
21. Agenzia Spaziale Italiana (ASI): Nuova rete fiduciale nazionale GNSS dell'Agenzia Spaziale Italiana (2026). https://www.asi.it/2021/11/completata-la-nuova-rete-fiduciale-nazionale-gnss-dellagenzia-spaziale-italiana/. Last Accessed 1 Mar 2026
22. Takasu, T.: RTKLIB: An open source program package for GNSS positioning (2026). http://www.rtklib.com. Last Accessed 1 Jan 2026
23. SARNET: Web server of the Sardinian Permanent GNSS Network (2025). https://www.sarnet.it/servizi.html. Last Accessed 1 Jan 2026